

# Numerical Simulation of Micropeening of quenched and tempered AISI 4140

A. Erz<sup>1</sup>, A. Klumpp<sup>1</sup>, J. Hoffmeister<sup>1</sup>, V. Schulze<sup>1</sup>

<sup>1</sup> Institute of Applied Materials (IAM – WK), Karlsruhe Institute of Technology, Germany

## Abstract

Numerical simulation of machining processes is a valuable tool for describing and optimizing those processes. In shot peening, numerical simulation is used to predict the residual stress distribution for instance. Due to the huge computing effort required for these simulations, a few years ago only a limited amount of shots could be simulated in a reasonable amount of time. For the simulation of micro-peening however, a much higher amount of shots needs to be considered to represent the process. With the availability of better and more efficient hardware at lower costs, it is now possible to simulate more than 1000 shots without having to accept extremely long computation times.

Based on existing simulation models for macro shot peening, new models were created for micro shot peening. The process conditions in micro-peening are different from macro peening, which had to be considered. Comparing the first numerical results to experimental results a qualitative agreement is shown. In order to achieve accordance quantitatively, further optimization of the description of the work piece material AISI 4140 (German grade 42CrMo4) is required to respect the circumstances that occur in micro-peening. That includes very high strain rates, an extreme deformation degree that is concentrated in the first few microns below the surface, as well as the possibility of generation of subgrains or grain refinement. Especially grain refinement has a huge impact on the local material behavior which has not been considered up to date. The optimized and extended material model for AISI4140 now considers also the microstructural changes that occur during the process. It is now possible to achieve a better correlation with experimental data and to predict the surface state with respect to residual stresses and also considering grain size.

**Keywords** micro peening, mechanical surface treatment, residual stresses, grain refinement, AISI 4140

## Introduction

Mechanical surface treatments, like shot peening and roller burnishing, induce strain hardening and compressive residual stresses, which both increase the fatigue life of components. These processes are well-established and widely used on parts that are exposed to cyclic loads. Micro-peening is a special form of shot peening, where a very small shot size is used (smaller than 100  $\mu\text{m}$  [1]) in comparison to standard shot peening. The shot material is also different: for this study, glass beads were used. The shots are accelerated by compressed air and velocities of up to roughly 200 m/s can be reached at 7 bar blasting pressure. Thus, the process conditions are not comparable to standard shot peening and naturally, the results are completely different. Usually a short penetration depth combined with a steep gradient can be observed in experiments regarding residual stresses. In addition, due to the small, low density shots, roughness is not increasing as much as in the standard shot peening process. This makes micro-peening an ideal surface treatment process for thin components. The process can also induce grain refinement, down to nanocrystalline scale in addition to residual stresses and strain hardening. These nanocrystalline surface layers are also beneficial for fatigue life, which can be seen in the extreme enhancement of the endurance limit of micro-peened components. In this paper, the micro-peening process is studied numerically with respect to both the classic approach regarding residual stresses and strain hardening, as well as taking grain refinement into account.

Geometry Model

A fully parameterized 3D-model is used as a geometry-model. Only a small cutout of size  $0.25 \times 0.25 \times 0.25 \text{ mm}^3$  is modeled to keep the element count as low as possible. The element type is C3D8R and half-infinite elements were connected to the free faces. These half-infinite elements serve for dampening the stress waves that otherwise would be reflected at the free faces. The model with shots arranged above the impact area is shown in Fig. 1.

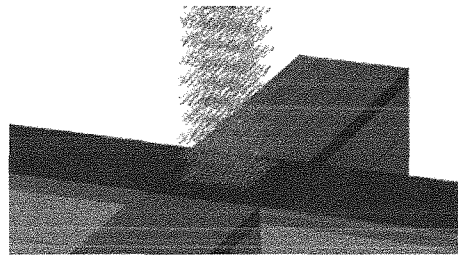


Fig. 1 – Geometry model for the shot peening simulation with shots arranged above the impact area

The shots are distributed randomly and thus represent the stochastic impacts during shot peening. The shots are generated with a script that considers the spatial distance between two shots that impact at the same time, as well as the time gap between two shots that impact in the vicinity of each other. The number of shots, angle, size and speed can be chosen freely. The shot count is only limited by the increasing simulation time. The evaluation of residual stresses requires the consideration of residual stress redistribution when material is removed during experimental X-ray measurement. Therefore, a subsequent layer removal is implemented in the simulation, which occurs at the end of the simulation after the peening process. The removal of a circular area is used in this study, which leads to a better comparability of the experimental process than the removal of an element layer as whole. The boundary conditions for the simulations presented in this work are kinematic coupling for the faces, while the bottom of the model was constraint in z-direction.

### Material Model

The necessity of strain-rate dependent material models in shot-peening simulations was shown by [2]. In body-centered cubic materials, changes in strain-rate and temperature mainly affect the yield strength, whereas strain hardening remains similar in a wide range of temperature and strain-rate [3, 4]. This effect allows for modeling the thermal flow stress part independently from hardening. The influence of the adopted constitutive description of hardening was discussed by several authors in literature [5–7]. [6] investigated the influence of purely isotropic and purely kinematic hardening in shot peening simulations and observed a distinct overestimation of the surface residual stresses if solely isotropic hardening is applied. Since shot peening induces an inhomogeneous cyclic deformation of the work piece surface, kinematic hardening should be applied to take account for the Bauschinger effect. An elastic-viscoplastic material model for FEM simulations, taking these effects into account, was presented by [4] and has proven to be suitable for the deformation simulation of several body-centered cubic materials. A similar material model including combined isotropic and kinematic hardening was used by [7] at a shot peening simulation of AISI 4140. This model was adopted and subsequently modified for the simulation of micropeening.

Grain refinement is implemented using a Zener-Hollomon approach, where the resulting grain size  $d$  is related to the Zener-Hollomon Parameter  $Z$  [8] (Eq. 1):

$$Z = \dot{\epsilon} \cdot e^{\frac{Q}{RT}}, \quad d = \alpha Z^m \quad (1)$$

where  $Q$  is the apparent activation enthalpy,  $R$  the universal gas constant,  $\dot{\epsilon}$  the strain rate and  $T$  the temperature in  $K$ .  $m$  and  $\alpha$  are material constants. Since Eq. 1 describes the

steady state condition, an incremental Avrami-approach was implemented. The fraction of recrystallized material  $X_r^{n+1}$  is expressed by Eq. 2:

$$X_r^{n+1} = 1 - \exp[-G(\varepsilon_{pl}^* + d\varepsilon_{pl} - \varepsilon_{crit})^p] \quad (2)$$

with the velocity constant  $G$ , the equivalent plastic strain  $\varepsilon_{pl}^*$ , the plastic strain increment  $d\varepsilon_{pl}$ , the critical strain  $\varepsilon_{crit}$  and an exponent  $p$  [8]. The equivalent plastic strain is the plastic strain that would have been necessary for the grain refinement that leads to the average grain size at increment  $i$ , under current strain rate and temperature conditions (Eq. 3):

$$\varepsilon_{pl}^* = \ln\left[-\frac{d - d_{av}}{G(d - d_0)}\right]^{\frac{1}{p}} \quad (3)$$

with the grain size  $d$  at steady state calculated by the Zener-Hollomon approach and the current average grain size  $d_{av}$ . The resulting average grain size at the end of the increment  $d_{av}^{n+1}$  is calculated from the recrystallized material fraction and the steady state grain size as shown in Eq. 4:

$$d_{av}^{n+1} = X_r^{n+1} \cdot d + (1 - X_r^{n+1}) \cdot d_0 \quad (4)$$

with the fraction of recrystallized material  $X_r^{n+1}$  (see Eq. 2), the grain size at steady state  $d$  calculated according to Eq. 1 and the initial grain size before recrystallization  $d_0$ .

## Results and Discussion

The cyclic material behavior was validated by using a 1-element model. Simulation and experimental results are compared for strain amplitudes of 1.5 % and 2.5 % in Fig. 2. The simulation results show very good accordance with the experimental results. The softening behavior in the first cycle is described by utilizing two isotropic hardening variables.

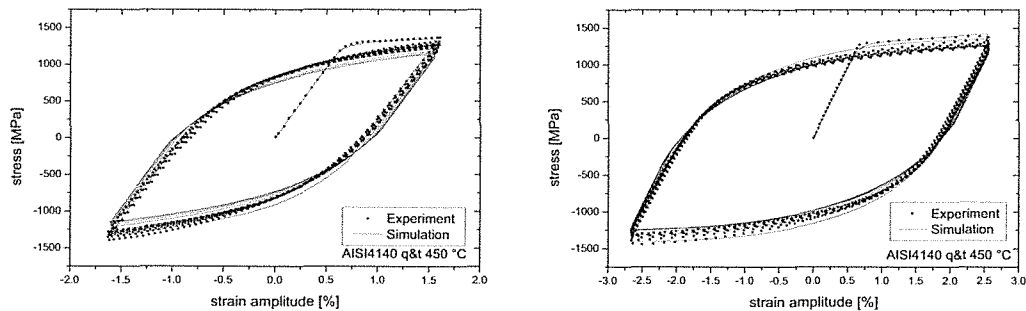


Fig. 2 – Cyclic material behavior, comparison between experiment and simulation

The temperature and strain-rate dependency of the flow stress is shown in Fig. 3. The athermal flow stress is temperature dependent and modelled according to [9]. The thermal flow stress was fitted using experimental results at  $\dot{\varepsilon} = 10^{-4}$  1/s and  $\dot{\varepsilon} = 10^{-3}$  1/s (Fig. 3 left). Effects of strain ageing can be noticed for temperatures higher than 300 K. The good accordance of the model with experimental results at higher strain rates can be seen in Fig. 3 (right).

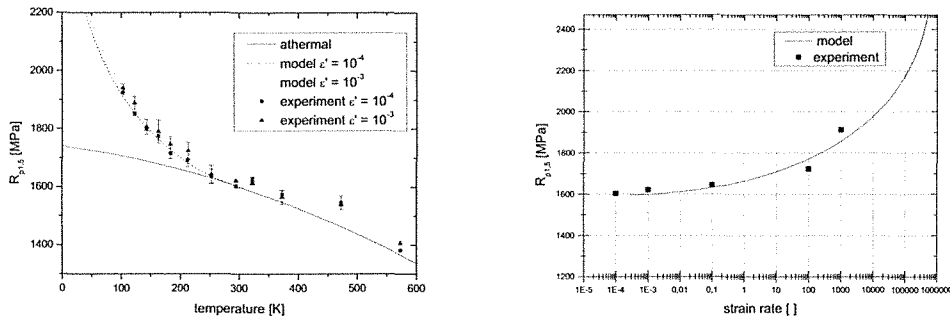


Fig. 3 – Strain rate dependency of the flow stress

The influence of shot size, shot speed and coverage on the residual stress state and resulting grain size has been investigated with the shot peening model. Shot sizes of 30, 40 and 50  $\mu\text{m}$  were used in order to have comparable sizes as used in the experiments. Although the blasting medium was denoted as 20-30  $\mu\text{m}$  by the manufacturer, it was found that it contains shots bigger than 30  $\mu\text{m}$ . [10] has shown that only the largest shots matter in terms of generating residual stresses. The effect on grain size, however, has not yet been investigated. For the shot speed, 105 m/s and 195 m/s were used, which corresponds to the measured shot speed at a blasting pressure of 1.5 bar and 7 bar respectively. The influence of the coverage was investigated by simulating different amounts of shots impacting on the same area of 0.2\*0.2 mm<sup>2</sup>. 500, 1000 and 1500 shots have been used for this, what corresponds to a coverage of roughly 300 %, 600 % and 900 %.

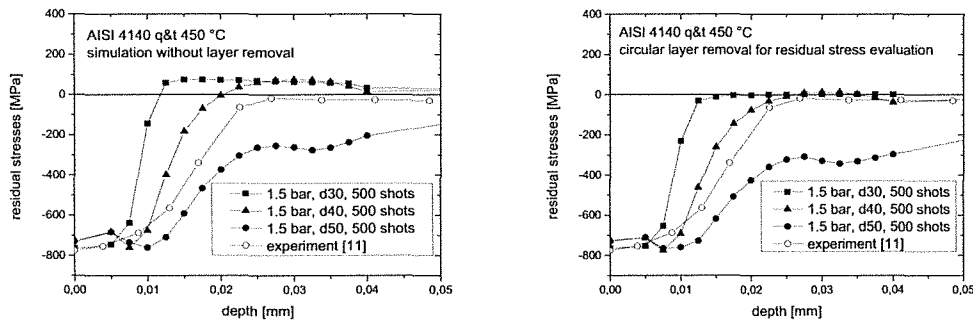


Fig. 4 – Residual stress depth distribution from simulation and experiment, without (left) and with (right) consideration of residual stress redistribution

The influence of shot size is shown in Fig. 4. While the surface residual stresses are mostly independent from the shot size, the depth of the zero crossing is increased with shot size. Shot sizes of 40 and 50  $\mu\text{m}$  exhibit a local minimum of residual stresses below the surface. The effect of residual stress redistribution on the resulting residual stress distribution becomes apparent by comparing the two diagrams of Fig. 4. The zero crossing is shifted to greater depths and the stresses do not change to tension after they reach zero. Overall, a better agreement with the experiments is achieved, especially for a shot diameter of 40  $\mu\text{m}$ . The simulation for a shot diameter of 50  $\mu\text{m}$  is largely overestimating the residual stresses below a depth of 0.02 mm, while showing a second plateau.

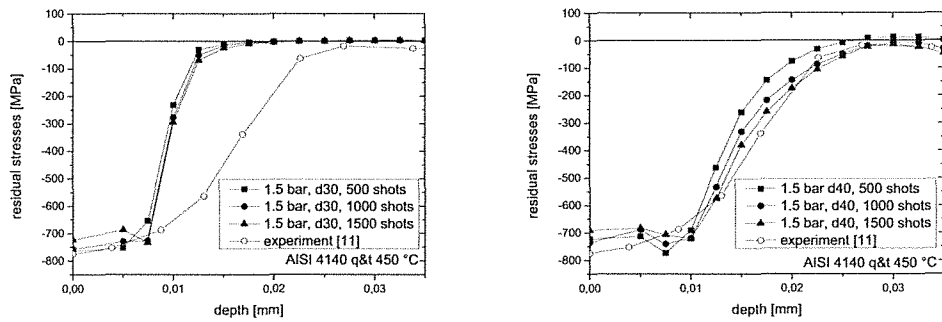


Fig. 5 – Influence of coverage on residual stress distribution at 1.5 bar blasting pressure for a shot diameter of 30  $\mu\text{m}$  (left) and 40  $\mu\text{m}$  (right)

The influence of coverage at 1.5 bar blasting pressure is shown in Fig. 5. For a shot size of 30  $\mu\text{m}$ , there already seems to be a saturation since almost no influence of the coverage is visible. A shot count of 1500 seems to produce a marginal cyclic softening effect at the near surface region. It is unlikely that an increasing shot count will reach match the residual stress profile which was determined in the experiment. A shot size of 40  $\mu\text{m}$  shows a minor effect of coverage on the residual stress distribution. Increasing coverage leads to a lower surface residual stress, as observed for the smaller shot size of 30  $\mu\text{m}$ . Slightly increased residual stresses and a smaller gradient of residual stresses are present in greater depths. Overall, a very good accordance with the experiment is achieved, although the total coverage in the experiment is much higher with around 100,000 impacts in that area. This might be due to the fact, that only the largest shots have an influence on the residual stress profile, so coverage in this case is coverage of the largest size-fraction, which greatly reduces the impacts of interest. Besides, coverage only has a marginal effect, as already shown.

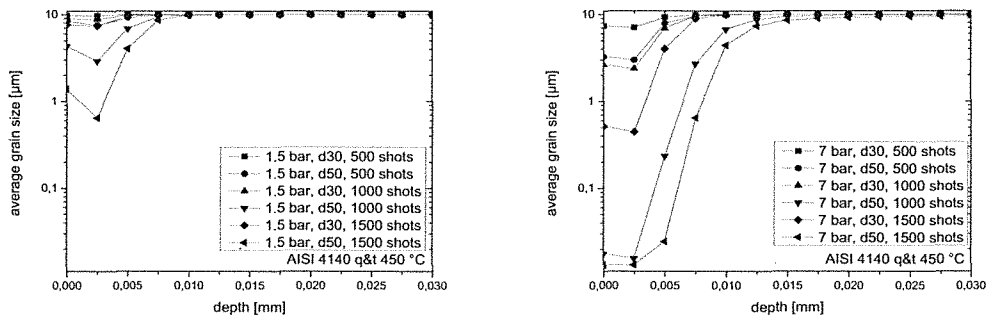


Fig. 6 – Grain refinement, simulation results at 1.5 bar (left) and 7 bar (right)

The effect of the considered process parameters on grain size is different from the residual stresses (compare Fig. 6). At 1.5 bar blasting pressure, the degree of grain refinement is clearly dependent on both shot size and coverage. For 500 and 1000 shots, there is almost no grain refinement visible, while 1500 shots induce minor grain refinement. The depth effect does not increase with coverage. At 7 bar blasting pressure, saturation in grain refinement is beginning for both shot sizes at an amount of 1000 shots, there are varying grain refinements for all shot sizes and shot counts. Higher coverage might still be more effective in terms of grain refinement, as observed in experiments. Comparing these results to experimental results, the depth effect is in good accordance (see Fig. 7), and the degree of grain refinement is in the correct magnitude, although it is hard to determine the actual grain size in the experiment. Currently, the simulation of grain size evolution still contains some extrapolation. Further experimental studies are needed in order to obtain a broad set of data for fitting.

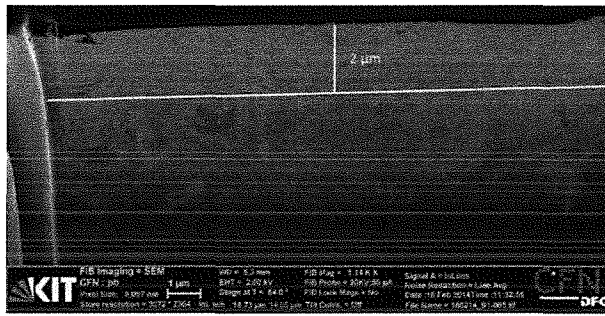


Fig. 7 – FIB cross section of the refined near surface grain structure after micro-peening

## Summary

It was shown that the material model approach is able to describe the material behavior in an adequate way. Characteristics like strain-rate dependency, cyclic softening and grain refinement are considered by the material model. The shot peening model is capable of handling up to 1500 shots in reasonable time and the results are in good accordance with the experiments. The influence of different process parameters on both residual stresses and grain size were investigated with the numerical model, and general rules could be deduced. Especially the shot size is of great importance when it comes to micro peening, since small variations have a huge impact on the resulting residual stress distribution.

## References

- [1] R. Weingärtner, J. Hoffmeister and V. Schulze, *Generation and Determination of Compressive Residual Stresses of Short Penetration Depths*, Materials Science Forum (2013), Vol. 768–769, pp. 580–586.
- [2] B.L. Boyce, X. Chen, J.W. Hutchinson and R.O. Ritchie, *The residual stress state due to a spherical hard-body impact*, Mech. Mater. 33 (2001), pp 441-454.
- [3] E. Macherauch and O. Vöhringer, *Das Verhalten metallischer Werkstoffe unter mechanischer Beanspruchung*, Materialwissenschaft und Werkstofftechnik 9 (1978), Nr. 11, pp. 370-391
- [4] G.Z. Voyiadjis and F.H. Abed, *A coupled temperature and strain rate dependent yield function for dynamic deformations of bcc metals*, International journal of plasticity 22 (2006), Nr. 8, pp. 1398-1431
- [5] S.T.S. Al-Hassani, *Mechanical aspects of residual stress development in shot peening*, ICSP1 (1981)
- [6] E. Rouhaud, A. Ouakka, C. Ould, J.-L. Chaboche and M. Francois, *Finite elements model of shot peening, effects of constitutive laws of the material*, Proceedings of the 9th International Conference on Shot Peening ICSP-9 (2005)
- [7] M. Klemenz, V. Schulze, I. Rohr and D. Löhe, *Application of the FEM for the prediction of the surface layer characteristics after shot peening*, Journal of Materials Processing Technology 209.8 (2009), pp. 4093-4102
- [8] J. Yanagimoto, K. Karhausen, A.J. Brand and R. Kopp, *Incremental Formulation for the Prediction of Flow Stress and Microstructural Change in Hot Forming*, Transactions of the ASME (1998), Vol. 120, pp. 316-322
- [9] F. Richter, *Physikalische Eigenschaften von Stählen und ihre Temperaturabhängigkeit: Polynome und graphische Darstellung*, Mitteilung aus dem Forschungsinstitut der Mannesmann AG, Stahleisen (1983)
- [10] M. Zimmermann, *Numerische und experimentelle Untersuchungen zur Randschichtausbildung beim Druckluft- und Ultraschallkugelstrahlen von IN718*, Dissertation Universität Karlsruhe, Shaker Verlag (2009)
- [11] R. Weingärtner, J. Hoffmeister and V. Schulze, *Investigation on the mechanisms improving fatigue strength in surface layers after micropeening*, ICSP12 (2014)